The Eurasia Proceedings of Science, Technology, Engineering and Mathematics (EPSTEM)
ISSN: 2602-3199

The Eurasia Proceedings of Science, Technology, Engineering and Mathematics (EPSTEM), 2026

Volume 39, Pages 9-18

IConTech 2026: International Conference on Technology

# A Comparative Study of Controller Performance in Five-Phase Induction Motor Drives

**Taieb Bessaad**
Hassiba Benbouali University of Chlef

**Maamar Latrouche**
Hassiba Benbouali University of Chlef

**Aicha Aissa Bokhtache**
Hassiba Benbouali University of Chlef

**Azzedine Khati**
Hassiba Benbouali University of Chlef

**Khedidja Benaicha-Mati**
Hassiba Benbouali University of Chlef

**Abstract**: In many applications where lowering the per-phase power draw while maintaining high system reliability is crucial, multiphase machines are increasingly seen as an attractive alternative to traditional three-phase machines. This trend has been strongly supported by recent research in the field. Fuzzy control techniques have proven effective for handling complex systems, but they often struggle when parameters change significantly over a broad range. Our work tackles this limitation through an adaptive fuzzy controller. In the context of vector-controlled induction motor drives and a five-phase asynchronous machine, the proposed approach deploys a control behavior model (CBM) to ensure robust performance even under abrupt load changes, rotor resistance variations and altered rotor inertia. Simulation results confirm that the adaptive fuzzy controller outperforms both standard fuzzy logic control and classical controllers, particularly in extreme parameter cases (e.g., $R_r = 200\ \% R_{rn}$, $L_m = 0.8 \times L_{mn}$ and $J = 200\ \% J{=}n$).

**Keywords:** Five-phase asynchronous motor, Indirect vector control, Control behavior model, Fuzzy control, Adaptive fuzzy control, Robustness

## Introduction

The adoption of multiphase machines has surged in recent years as power levels increase and high-reliability electrical applications demand better distribution of power by using more than three phases (Yepes et al., 2022; Kulandaivel et al., 2023). In addition to efficient power sharing, multiphase machines bring several noteworthy advantages: they allow lower phase voltages without raising phase currents, they reduce iron losses and torque ripple, increase the torque ripple frequency, and deliver improved fault tolerance (Laksar et al., 2021; Yepes et al., 2022). Thanks to these benefits, multiphase machines are increasingly found in high-power contexts such as wind generation, more-electric aircraft, ship propulsion and mining systems (Kulandaivel et al., 2023).

Despite their promise and intrinsic robustness, controlling multiphase machines is inherently more challenging than controlling DC machines because their mathematical models are highly nonlinear and strongly coupled (Duran et al., 2008; Xue, 2023). As a result, advanced control methods are required. Modern control approaches such as state-feedback control, direct torque control (DTC), vector control and adaptive control are now

commonly employed (Hosseyni et al., 2018; Mehedi et al., 2017). While traditional PI controllers remain popular due to their simplicity, their performance degrades under large parameter shifts or external disturbances (Elbarbary et al., 2024; Belhamdi & Goléa, 2021). To address these limitations, intelligent control frameworks—including sliding mode control, fuzzy logic, neural networks and adaptive schemes—have been increasingly used (Tidke & Chowdhury, 2024; Bouzidi, 2024). Integrating adaptive control with robust fuzzy logic offers a more resilient solution and better tracking under uncertainty (Bessaad, 2019; Sumukh et al., 2025).

The objective of this study is to address these challenges by combining an adaptive scheme with a robust fuzzy logic controller, thereby enhancing overall performance and ensuring robustness even when machine parameters vary significantly. The aim of this work is to overcome this limitation, integrating adaptive control with the robust fuzzy controller offers a promising solution to enhance overall control performance and ensure stability, even in the face of significant parameter variations.

## Model of an Induction Machine

The induction-machine model can be expressed using a state-space representation (Arahal et al., 2018). For a five-phase machine, the mathematical model is defined in the arbitrary reference frame d–q–x–y–o. Within this frame, the d and q axes handle the flux generation and torque production processes, while the x and y axes represent the loss-producing subspaces. The zero (o) component serves to preserve the total power balance within the system. The decoupling (transformation) matrix for the five-phase machine is formulated as shown by Chikondra et al. (2023).

$$A=\sqrt{\frac{2}{5}}\begin{bmatrix} 1 & \cos(\frac{2\pi}{5}) & \cos(\frac{4\pi}{5}) & \cos(\frac{4\pi}{5}) & \cos(\frac{2\pi}{5}) \\ 0 & \sin(\frac{2\pi}{5}) & \sin(\frac{4\pi}{5}) & \sin(\frac{4\pi}{5}) & \sin(\frac{2\pi}{5}) \\ 1 & \cos(\frac{4\pi}{5}) & \cos(\frac{8\pi}{5}) & \cos(\frac{8\pi}{5}) & \cos(\frac{4\pi}{5}) \\ 0 & \sin(\frac{4\pi}{5}) & \sin(\frac{8\pi}{5}) & -\sin(\frac{8\pi}{5}) & -\sin(\frac{4\pi}{5}) \\ \frac{1}{\sqrt{2}} & \frac{1}{\sqrt{2}} & \frac{1}{\sqrt{2}} & \frac{1}{\sqrt{2}} & \frac{1}{\sqrt{2}} \end{bmatrix} \tag{1}$$

$$\begin{cases} \delta L_S \frac{d}{dt} i_{sd} = -\left( R_S + \frac{L_m^2}{L_r} R_r \right) i_{sd} - \delta L_S \omega_S i_{sq} - \frac{L_m}{T_r L_r} \phi_{rd} \\ \qquad\qquad + v_{sd} \\ \delta L_S \frac{d}{dt} i_{sq} = -\left( R_S + \frac{L_m^2}{L_r} R_r \right) i_{sq} - \delta L_S \omega_S i_{sd} - \frac{L_m}{L_r} \omega_r \phi_{rd} \\ \qquad\qquad + v_{sq} \\ \frac{d}{dt} \phi_{rd} = \frac{L_m}{T_r} i_{sd} - \frac{1}{T_r} \phi_{rd} \\ \frac{d}{dt} \phi_{rq} = \frac{L_m}{T_r} i_{sq} - (\omega_S - \omega_r) \phi_{rd} \\ T_{em} = p \frac{L_m}{T_r} \left( \phi_{rd} i_{sq} - \phi_{rq} i_{sd} \right) \\ J \frac{d}{dt} \Omega = T_{em} - T_L - f\Omega \end{cases} \tag{2}$$

In which rotor time constant is $T_r = \frac{L_r}{R_r}$; the total leakage is $\delta = 1 - \frac{L_m^2}{L_S L_S}$ ; $\phi_{rd}$ is rotor flux relative to axis $d$ ($\phi_{rd}$ = $\phi_r$ for rotor field-oriented control); $\phi_{rq}$ is rotor flux relative to $q$- axis ($\phi_{rq}$ = 0) ; $i_{sd}$ is stator relative current to the $d$- axis ; $i_{sq}$ is stator relative current to the $q$- axis ; $Tem$ is electromagnetic torque; $s,r$ are indices relating to the stator and rotor; $L_s$ , $L_r$ are inductance of stator and rotor windings respectively ; $L_m$ is mutual inductance; $J$ is inertia moment ; $p$ is number of pole pairs ; $K_f$ is Friction coefficient; $\Omega$ is electrical rotation speed.

In Fig. 1, one note the appearance of vector control blocks where PI controller is used for the two stator currents and the speed along the *d* and *q* axes then one replace this controller with FLC and BMC controller.

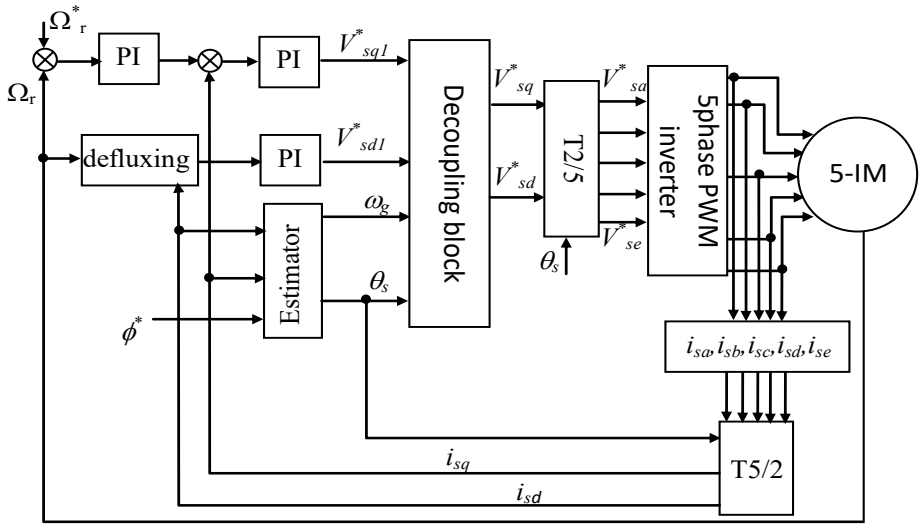


Figure1. A control method for a five-phase motor drive, utilizing an indirect rotor flux orientation technique.

## Behavior Model Control Principles

In this article, the functions P(s) and M(s) are employed to represent, respectively, the plant (process) and its mathematical model. The Behavior Model Control (BMC) strategy enhances the control algorithm's effectiveness by incorporating supplementary control signals (Derugo, 2017). This method uses both a primary controller, denoted (FCp(S)) and an additive controller, (FCr(S)). The overall control structure is illustrated in Figure 2 (Morawiec et al., 2019).

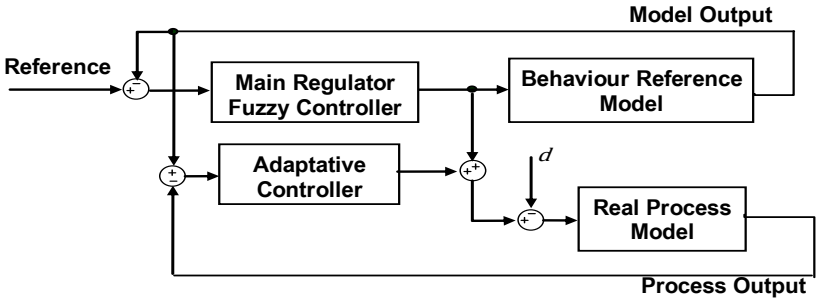


Figure 2. Structure of CBM (Control Behavior Model)

Note that the principal controller eliminates the error is calculated as the difference between the reference value $Y_{ref}$ and the output value, which can be either the model output or the process output $Y_{mod}$ or a process $Y$. Therefore, it is possible to define two CBM structures: first based on the output of the real process model, and a second based on an imposed model output. We can derive the following expressions (Fei et *al.*, 2018) based on the information presented in Figure 2, can be derived:

The main controller produces a control signal, $u_{reg}$ , based on the reference value $Y_{ref}$.. This signal is then fed into a predefined behavior model, $F_M(S)$, which generates an output $Y_{mod}$ . The difference between the model $Y_{mod}$ and the actual process output $Y$ is used by a secondary regulator, known as the adaptation controller, to compute an additional control signal, $\Delta u_{reg}$. By keeping the error ($Y - Y_{mod}$), constant, the process behavior aligns with the imposed model, which is the essence of behavior model control. The extra control $\Delta u_{reg}$ is combined with the main controller output $u_{reg}$ and applied to the real process $F_P(S)$.

This complementary control enhances the robustness of the overall system, allowing the imposed behavior to be maintained even in the presence of disturbances (Keighobadi et al., 2018). Furthermore, this approach enables

the linearization of nonlinear systems through the use of a linear reference model (Shihabudheen et al., 2018). It is important to note that the primary controller calculates the error as the difference between the reference YrefY_{\text{ref}}Yref and the output, which can either be the model output YmodY_{\text{mod}}Ymod or the process output YYY. Accordingly, two types of CBM structures can be defined: one based on the actual process output, and another based on the output of the imposed model. The corresponding expressions can be derived from the information shown in Figure 2 (Fei et al., 2018)

$$\begin{cases} Y(S) = \left[u_{reg}(S) + \Delta u_{reg}(S) - d\right] F_P(S) \\ \Delta u_{reg}(S) = \left[F_M(S) + u_{reg}(S) - Y(S)\right] F_{Cc}(S) \end{cases} \tag{3}$$

The system that expresses both the process output ($Y$) and the model output ($Y_{mod}$) is reached after the calculation as:

$$\begin{cases} Y(S) = \dfrac{F_P(S)(1 + F_M(S).F_{Cc}(S))}{1 + F_P(S).F_{Cc}(S)} u_{reg}(S) \\ \qquad\quad - \dfrac{F_P(S)}{1 + F_P(S).F_{Cc}(S)}.d \\ Y(S) = F_M(S).u_{reg}(S) \end{cases} \tag{4}$$

Where the disruption is denoted by $d$.

The following presumptions must be met by the behavior corrector $C_C(S)$:

$$\begin{cases} \left|F_M(S).F_{Cc}(S)\right| >> 1 \\ \left|F_P(S).F_{Cc}(S)\right| >> 1 \end{cases} \tag{5}$$

Simplifying results in the following:

$$\begin{cases} Y(S) = F_M(S).u_{reg}(S).\dfrac{1}{F_{Cc}(S)}.d \\ Y_{mod}(S) = F_M(S).u_{reg}(S) \end{cases} \tag{6}$$

The result of this is as follows:

$$Y(S) = Y_{mod}(S) - \frac{1}{F_{Cc}(S)}.d \tag{7}$$

At low disturbance, the process output ($Y$) and model output ($Y_{mod}$) are identical. If this disturbance is minimal in comparison to ($Y$) process output, it precisely corresponds to ($Y_{mod}$) model's output. These terms are written:

$$\frac{d}{F_{Cc}(S)} << F_M(S).u_{reg}(S) \tag{8}$$

When the return from the model output $Y_{mod}$ is taken into account, the system (3) becomes:

$$\begin{cases} Y_{\text{mod}}(S) = \dfrac{F_M(S).F_{Cp}(S)}{1+F_M(S).F_{Cp}(S)}.Y_{ref}(S) \\ Y(S) = \dfrac{F_P(S)(1+F_M(S).F_{Cc}(S))}{F_M(S)(1+F_P(S).F_{Cc}(S))}.Y_{mod}(S) \\ \quad -\dfrac{F_P(S)}{1+F_P(S).F_{Cc}(S)}.d \end{cases} \tag{9}$$

Let's assume the following situation to simplify the transfer function:

$$\left|F_M(S).F_{Cc}(S)\right| >> 1 \tag{10}$$

## Controller of Speed Loop

The input variables E and ΔE, along with the output variables, are represented by conventional triangular-shaped membership functions. Stator speeds are classified into seven fuzzy sets, while for stator currents, each membership is segmented into three fuzzy sets, as illustrated in Figure 4. The Center of Area (COA) approach is used to carry out the defuzzification process, and Mamdani (Max-Min) is the inference method used (Zhang et *al.*, 2021). The speed loop correction controller is employed to eliminate the difference between the machine's actual speed and the reference speed $\Omega_{mod}$ provided by the model. To achieve this, the controller uses both the error and its derivative as inputs. The resulting correction signal, $T_{em}$, which guides the five-phase machine to follow the model's behavior, is obtained by integrating the controller output (Arahal et al., 2018). The correction controller, denoted as FLCR (Figure 3), has a structure similar to that of a fuzzy logic main controller (FLC), consisting of three key components: a knowledge base, fuzzification (F), inference (I), and defuzzification (D). Here, the machine's speed $\Omega$ and stator currents ($i_{sd}$ and $i_{sq}$)are used as input variables $u$.

Both the error E and its change ΔE, along with the output variable, are described using conventional triangular membership functions. The stator speed is divided into seven fuzzy sets, whereas the stator currents are segmented into three fuzzy sets each, as shown in Figure 4. Defuzzification is carried out using the Center of Area (COA) method, and Mamdani's Max-Min approach is applied for inference (Zhang et al., 2021).

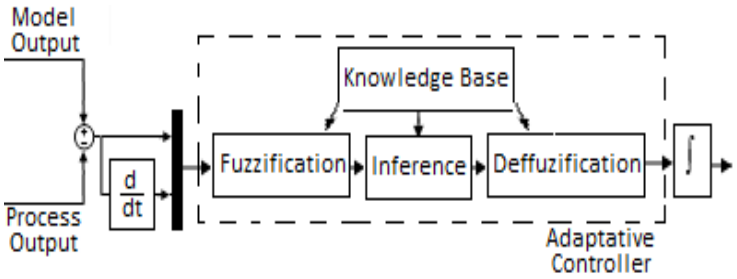


Figure 3. The fuzzy correction controller's structure FLCR

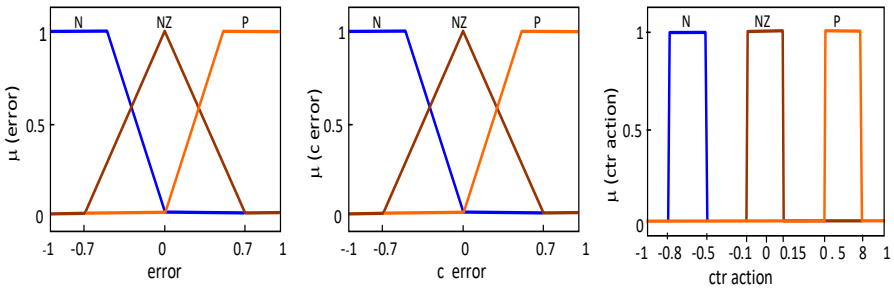


a

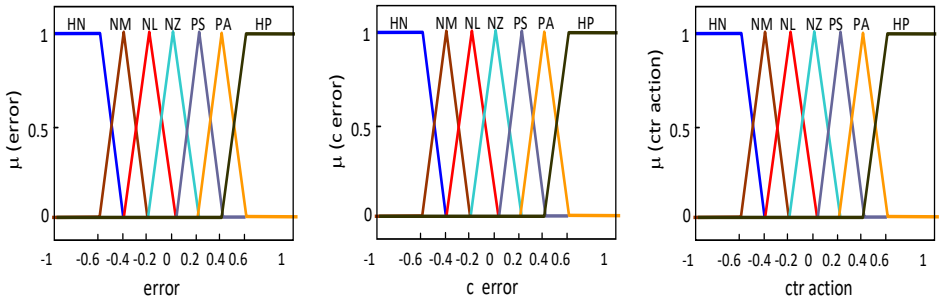


b

Figure 4. Input and output variables membership functions of representation:
a) Currents, b) Speed.

The following defines the various sets:
HN: High Negative;
PL: Positive low;
NZ: Near Zero;
NM: Negative Medium;
PA: Positive Average;
NL: Negative low;
HP: High Positive

## Results and Discussion

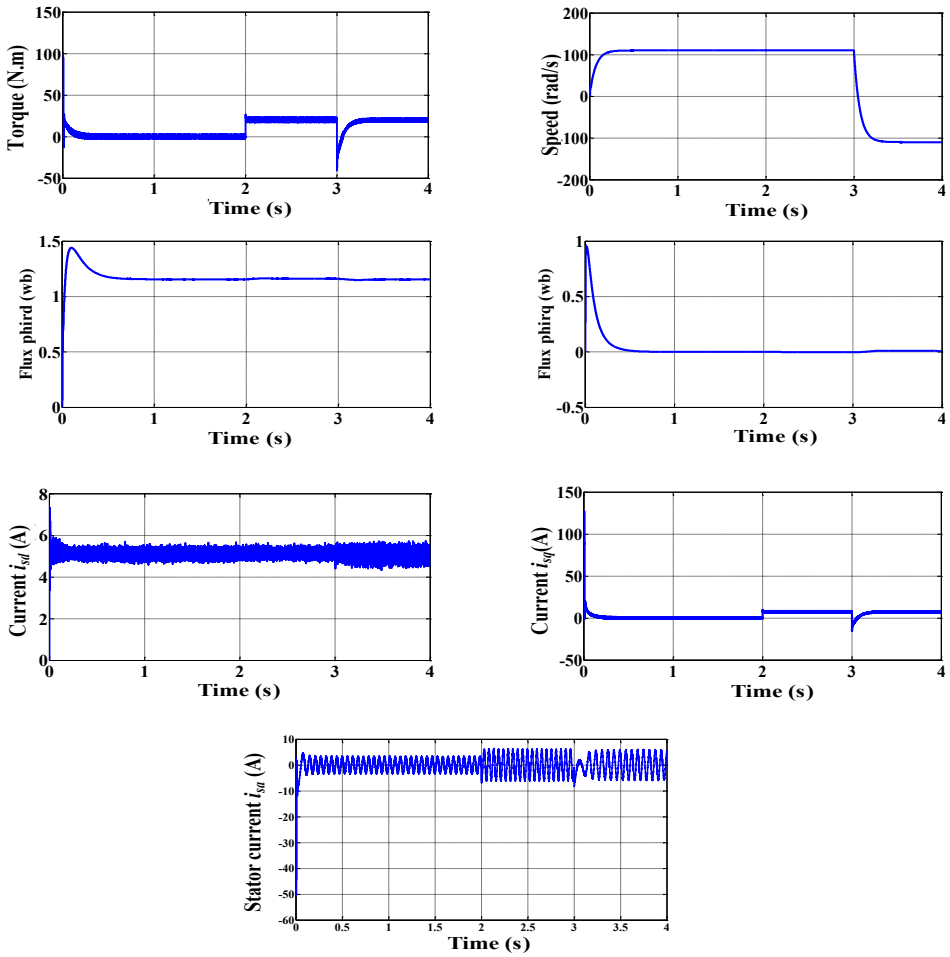


Figure 5. Performance of the 5-phase I.M with fuzzy adaptive regulators in indirect vector control during speed reversal

The simulations were executed within a MATLAB environment where the differential equations describing the dynamic behavior of the five-phase induction motor and its load were implemented. Figures 4 and 5 show the rotor speed, rotor flux magnitude, components of the currents ($i_{ds}$,$i_{qs}$), the flux, and the actual stator current $i_{as}$ as when using a PI regulator. To showcase the performance of the predictive control applied to speed regulation, the five-phase induction motor was simulated with a reference speed of 100 rad/s under no-load conditions. At t=1s a nominal load of 10 N·m was applied (Figure 6).

Figure 5 presents the system responses, such as stator currents, electromagnetic torque, and rotor speed. The results confirm that the dynamic performance of the five-phase induction machine is satisfactory. The simulation process was executed in two stages :

1. A start-up simulation under no-load conditions.
2. At t=2s a torque load of 20 Nm is applied, and at t=3s the rotation reverses direction from +110 rad/s to −110 rad/s.

The behavioral-model-control scheme for a five-phase induction machine is illustrated in Figure 5. The simulation is designed to show how an adaptive fuzzy controller (BMC) can regulate the machine's speed. The sequence begins with a no-load start, then at t=2s a 20 Nm load is applied, followed by a reversal of motion at t=3s from +110 rad/s to −110 rad/s. The response plots display the torque, stator current, and speed trajectories. It is clear that the system's dynamic behavior is acceptable.

## Robustness of the System

Figure 6 depicts the performance of a five-phase induction motor drive under conditions of variable load, doubled rotor inertia (200% $J_n$), rotor resistance at 100% of nominal ($R_{rn}$), and mutual inductance set to $0.8 \times L_{mn}$. The system is controlled using three strategies: behavior model control (CBM), fuzzy logic control (FLC), and a conventional PI controller.

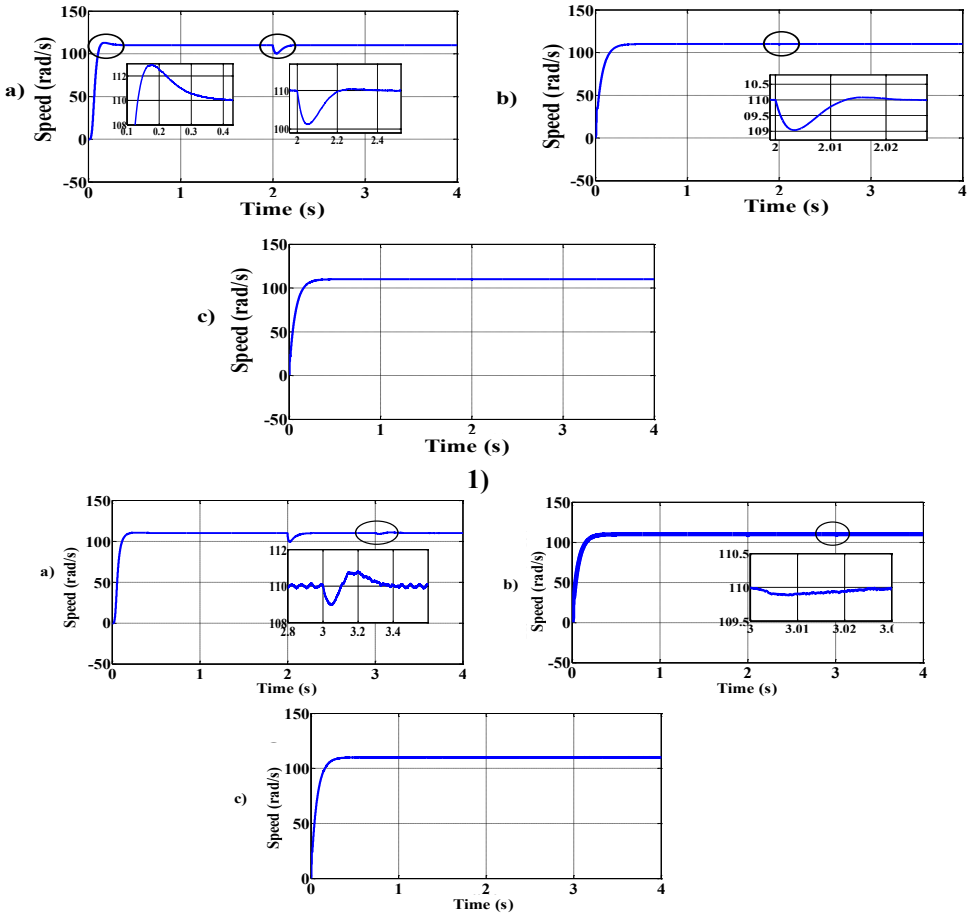

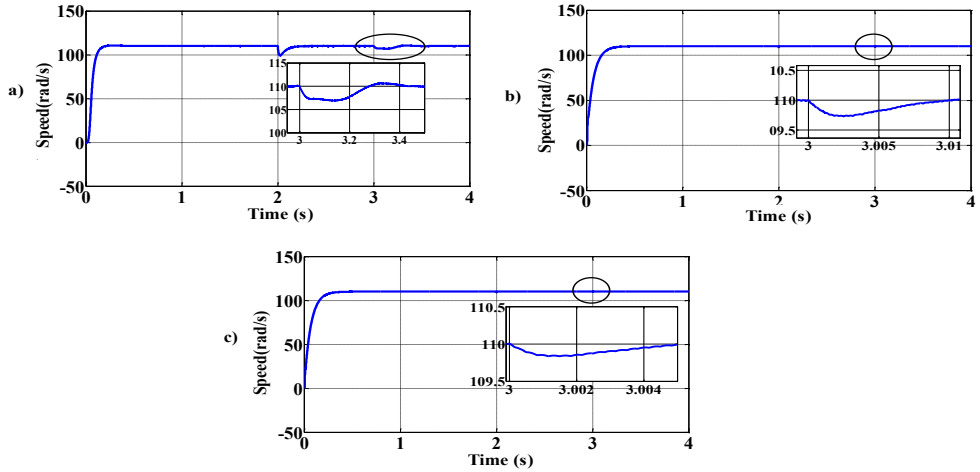


**3)**

Figure 6. Comparison between a) PI, b) FLC, c) BMC for: 1) Rotor inertia variation $J = 4*J_n$, 2) Variation of resistance $R_r$ ($R_r = 200\%R_{rn}$), 3) Inductance variation$L_m$ ($L_m = 0.8*L_{mn}$)

In Figure 6, the CBM clearly outperforms the other methods by showing reduced sensitivity to external disturbances. Notably, the CBM approach more effectively mitigates transient errors caused by disturbances, and the speed response displays no overshoot, minimal steady-state error, and fast disturbance rejection. As a result, the adaptive controller maintains the desired performance in the face of both internal and external parameter variations and disturbances.

## Conclusion

A five-phase asynchronous machine, powered by voltage, is controlled through indirect vector control with adaptive control implemented numerically. The proposed adaptive control uses a reference model with an adaptation mechanism running in parallel to the inner-loop fuzzy logic controller (FLC). The performance of the fuzzy adaptive controller was evaluated through simulations. The results indicate that the behavior model control (CBM) is highly robust against variations in load, rotor inertia (200% $J_n$), rotor resistance (100% $R_{rn}$), and mutual inductance (0.8 $L_{mn}$), outperforming both conventional FLC and PI controllers. Despite parameter changes and external disturbances, the system maintains the desired trajectory, and the speed response closely follows the reference model.

Future work will focus on developing a laboratory prototype to experimentally validate the simulations and exploring the potential of adaptive fuzzy controllers for a series-connected two-motor five-phase drive fed by a single five-leg inverter, proposed as a control strategy for traction systems.

## Induction Motor Data

Rated power $P_n$= 3kW, nominal currant $I_n$= 3.6/6.2A, stator resistance $R_s$= 2.5Ω, rotor resistance $R_r$=1.9Ω, stator inductance $L_s$= 0.24H, rotor inductance $L_r$= 0.24H, mutual inductance $L_m$= 0.226H, rated phase stator voltage $V_n$ = 380V, pole pair number $P$=2, rotor speed $N$ = 1499tr/min, viscous friction coefficient $K_f$= 0.0006Nms/rad, Rotor inertia $J$= 0.031kg.m2.

## Scientific Ethics Declaration

* The authors declare that the scientific ethical and legal responsibility of this article published in EPSTEM journal belongs to the authors.

* There is no need for any scientific ethics committee permission for this study.

## Conflict of Interest

* The authors declare that they have no conflicts of interest

## Funding

* This research received no specific grant from any funding agency in the public, commercial, or not-for-profit sectors.

## Acknowledgements or Notes

* This article was presented as an oral presentation at the International Conference on Technology (www.icontechno.net ) held in Budapest/Hungary on February 05-08, 2026.

* The authors would like to thank the conference scientific committee and referees for their feedback on the article.

## References

Arahal, M. R., Barrero, F., Duran, M. J., Ortega, M. G., & Martin, C. (2018). Trade-offs analysis in predictive current control of multi-phase induction machines. *Control Engineering Practice, 81*, 105–113.

Chikondra, B., AlZaabi, O., & Hosani, K. A. (2023). Direct torque control of five-phase induction motor drives with xy current regulation under an open-phase fault condition. In *Proceedings of the IEEE Energy Conversion Congress and Exposition (ECCE)* (pp. 4733–4736).

Derugo, P. (2017). Adaptive neuro fuzzy PID type II DC shunt motor speed controller with Petri transition layer. In *Proceedings of the 26th International Symposium on Industrial Electronics (ISIE)* (pp. 395–400).

Elbarbary, Z., Azeem, M. F., & Azazi, H. Z. (2020). Adaptive fuzzy-based IRFOC of speed sensorless six-phase induction motor drive system. *Journal of Circuits, Systems and Computers, 29*(4), 2050062.

Fang, J. F., & Hu, T. (2018). Adaptive backstepping fuzzy sliding mode vibration control of flexible structure. *Journal of Low Frequency Noise, Vibration and Active Control, 37*(4), 1079–1096.

Fei, J., & Cheng, L. (2018). Adaptive fractional order sliding mode controller with neural estimator. *Journal of the Franklin Institute, 355*(5), 2369–2391.

Fei, J., & Wang, T. (2018). Adaptive fuzzy-neural-network based on RBFNN control for active power filter. *International Journal of Machine Learning and Cybernetics, 10*(6), 1–12.

Ho, C. M., Dao, H. V., Tran, D. T., & Ahn, K. K. (2023). Design of observer-based adaptive fuzzy fault-tolerant control for pneumatic active suspension with displacement constraint. In *Proceedings of the International Conference on System Science and Engineering (ICSSE)* (pp. 184–189).

Keighobadi, J., Fateh, M. M., & Chenarani, H. (2018). Adaptive fuzzy passivation control based on backstepping method for electrically driven robotic manipulators. In *Proceedings of the 6th RSI International Conference on Robotics and Mechatronics (IcRoM)* (pp. 292–297).

Li, S., Yang, J., Wang, Y., & Yang, G. (2022). Dual closed-loop control strategy on harmonic plane for multiphase induction motor with harmonic injection based on air-gap flux orientation control. *IEEE Journal of Emerging and Selected Topics in Power Electronics, 10*(5), 6101–6111.

Morawiec, M., Strankowski, P., Lewicki, A., Guziński, J., & Wilczyński, F. (2019). Feedback control of multiphase induction machines with backstepping technique. *IEEE Transactions on Industrial Electronics, 67*(6), 4305–4314.

Narmada, A., Jain, A., & Shukla, M. K. (2024). Recurrent neural network based backstepping controller for Genesio-Tesi chaotic system. In *Proceedings of the Sixth International Conference on Computational Intelligence and Communication Technologies (CCICT)* (pp. 292–297).

Sala, G., Mengoni, M., Rizzoli, G., Degano, M., Zarri, L., & Tani, A. (2021). Impact of star connection layouts on the control of multiphase induction motor drives under open-phase fault. *IEEE Transactions on Power Electronics, 36*(4), 3717–3726.

Shihabudheen, K. V., Raju, S., & Pillai, G. N. (2018). Control for grid-connected DFIG-based wind energy system using adaptive neuro-fuzzy technique. *International Transactions on Electrical Energy Systems, 28*(5), e2526.

Zhang, Z., Wei, H., Zhang, W., & Jiang, J. (2021). Ripple attenuation for induction motor finite control set model predictive torque control using novel fuzzy adaptive techniques. *Processes, 9*(4), 710.

Zhou, D., Zhao, J., & Li, Y. (2016). Model-predictive control scheme of five-leg AC–DC–AC converter-fed induction motor drive. *IEEE Transactions on Industrial Electronics, 63*(7), 4517–4526.

## Author(s) Information

**Taieb Bessaad**
Hassiba Benbouali University of Chlef
Hssania Chlef, Algeria
ORCID: https://orcid.org/0009-0002-5018-5069
*Contact e- mail: *t.bessaad@univ-chlef.dz*

**Maamar Latrouche**
Hassiba Benbouali University of Chlef
Hssania Chlef, Algeria
ORCID: https://orcid.org/0000-0001-7800-2805

**Aicha Aissa Bothtache**
Hassiba Benbouali University of Chlef
Hssania Chlef, Algeria
ORCID: https://orcid.org/0000-0001-9659-0057

**Azzedine Khati**
Hassiba Benbouali University of Chlef
Hssania Chlef, Algeria
ORCID: https://orcid.org/0000-0003-3288-2768

**Khedidja Benaicha-Mati**
Hassiba Benbouali University of Chlef
Hssania Chlef, Algeria
ORCID: https://orcid.org/0009-0002-9161-4587

*Corresponding authors contact e-mail

**To cite this article:**

Bessaad, T., Latrouche, M., Aissa Bokhtache, A., Khati A., & Benaicha-Mati, K. (2026). A comparative study of controller performance in five-phase induction motor drives. *The Eurasia Proceedings of Science, Technology, Engineering and Mathematics (EPSTEM), 39,* 9-18.